

# 3D Scan Registration Using the Normal Distributions Transform with Ground Segmentation and Point Cloud Clustering

Arun Das,<sup>\*</sup> James Servos,<sup>\*</sup> and Steven L. Waslander<sup>†</sup>  
University of Waterloo, Waterloo, ON, Canada, N2L 3G1

**Abstract**—The Normal Distributions Transform (NDT) scan registration algorithm models the environment as a set of Gaussian distributions and generates the Gaussians by discretizing the environment into voxels. With the standard approach, the NDT algorithm has a tendency to have poor convergence performance for even modest initial transformation error. In this work, a segmented greedy cluster NDT (SGC-NDT) variant is proposed, which uses natural features in the environment to generate Gaussian clusters for the NDT algorithm. By segmenting the ground plane and clustering the remaining features, the SGC-NDT approach results in a smooth and continuous cost function which guarantees that the optimization will converge. Experiments show that the SGC-NDT algorithm results in scan registrations with higher accuracy and better convergence properties when compared against other state-of-the-art methods for both urban and forested environments.

## I. INTRODUCTION

Scan registration algorithms have a significant role in mapping algorithms for mobile robotics. Many sensors provide information about the environment in the form of point clouds, such as RGBD cameras, LIDAR and stereo cameras. Scan registration algorithms rely on overlapping geometry between scans to determine the relative transformation between the two scans. Knowing the transformation parameters allows for the aggregation of point cloud data, which is commonly required for autonomous operation in unknown environments.

The most common scan registration algorithm is the iterative closest point (ICP) algorithm. ICP was independently introduced by Besl and McKay [1], Chen and Medioni [2], and Zhang [3]. The ICP algorithm attempts to find transform parameters such that the Euclidean distance between nearest neighbour points are minimized. The ICP algorithm does not take into account the underlying surface of the point cloud, as it operates at the point level. Furthermore, ICP assumes that the two point clouds can overlap perfectly, however in practice this is not the case due to noise and the sampling characteristics of the sensor. To address the shortcomings of ICP, Segal et al. introduced generalized-ICP (G-ICP) [4], which calculates the surface normal at each point, using local neighbourhoods, and only includes correspondences between points of similar surface structure between the two scans. The main bottleneck of the ICP algorithm is the costly nearest neighbour search needed to identify points in the

local neighbourhoods, which is generally computationally expensive.

The normal distributions transform (NDT) is an alternative approach, first suggested by Biber and Strasser for scan registration and mapping in 2D [5]. It was later expanded for use with 3D point clouds by Magnusson et al. [6], and further expanded to a distribution-to-distribution registration problem by Stoyanov et al. [7]. The advantage of the NDT algorithm is that it does not need to explicitly compute the nearest neighbour correspondences because it represents the scan as a set of Gaussian distributions instead of as individual points. The NDT algorithm also represents the underlying scan as a set of Gaussian distributions that locally models the surface as a generative distribution. It is an optimization based approach that determines the transform parameters which maximize the likelihood of the scan being sampled from the NDT distribution.

The standard formulation of NDT results in a nonlinear optimization which is susceptible to poor convergence properties when starting from initial estimates that deviate significantly from the true transformation. The voxel based discretization of NDT generates Gaussian distributions which do not necessarily model the environment accurately. The distributions only locally model the points within each cell, and may not capture broader features present within the scan. Furthermore, the crossing of points between cell boundaries during the optimization process results in a cost function which is discontinuous. Previously, the authors [8] proposed multi scale k-means NDT (MSKM-NDT), which partitions a 2D laser scan using k-means clustering over multiple scales with a coarse-to-fine optimization method. Although the MSKM-NDT method avoids local minima, improves convergence, and results in a smooth and continuous cost function, the number of clusters must be known *a priori*.

Scan partitioning has also been performed in 3D by Moosmann et al., who used a graph based approach to segment a laser scan based on local convexity criterion [9]. The graph based method computes surface normal information in order to partition the scan, however good quality surface normal information is difficult to generate for sparse laser scans, or when the environment consists of objects such as trees, brush, and foliage. Douillard et al. demonstrated scan partitioning using Gaussian processes and incremental sample consensus applied to ICP scan registration, where correspondences between neighbouring points were constrained to belong to corresponding partitions [10].

The contribution of this work is the application of a seg-

<sup>\*</sup> M.A.Sc. Candidate, Mechanical and Mechatronics Engineering, University of Waterloo; adas@uwaterloo.ca, jdservos@uwaterloo.ca

<sup>†</sup> Assistant Professor, Mechanical and Mechatronics Engineering, University of Waterloo; stevenw@uwaterloo.ca

mentation and clustering algorithm to improve the accuracy and convergence of the NDT algorithm, specifically for open, outdoor environments with sparse point-clouds. Ground segmentation is performed in order to separate natural features in the environment which are typically separated by the ground. The natural features which represent the environment are used to generate Gaussian clusters for the NDT algorithm, which is desirable since it allows for accurate modelling of the environment using significantly fewer distributions compared to the standard NDT algorithm. The application of ground segmentation results in the decomposition of the environment into ground and obstacle partitions which can be used for higher level mission execution.

To achieve the decomposition, a ground segmentation algorithm based on Gaussian process regression [11] and incremental sample consensus [12] is applied to the 3D laser scan. A greedy clustering algorithm which partitions the non-ground points into clusters is then proposed. Assuming that the non-ground points are fully separated by the ground, the greedy clustering algorithm generates clusters which group together points belonging to segmented features in the environment, such as trees, bushes, etc. The segmented feature clusters are used to construct Gaussian distributions for the NDT algorithm. The NDT algorithm is modified to evaluate the cost function for all generated clusters, which guarantees that the nonlinear optimization is well defined and all standard nonlinear optimization algorithms will converge to a solution which satisfies the necessary conditions for optimality [13]. Evaluation at all Gaussian clusters is performed for both the point-to-distribution and distribution-to-distribution variants of the NDT algorithm. The proposed method is evaluated for accuracy and convergence using laser data obtained from the Ford campus data set [14] and a sparse forested park at Worcester Polytechnic Institute.

## II. PROBLEM FORMULATION

Scan registration algorithms seek to find the optimal transformation between two point cloud scans, a *reference scan* and a *scene scan*. The goal is to determine transformation parameters which best align the two scans such that they overlap as much as possible. Denote the reference scan as the set of points  $Y = \{y_1, \dots, y_{N_Y}\}$  where  $y_i \in \mathbb{R}^3$  for  $i \in \{1, \dots, N_Y\}$  and the scene scan as  $X = \{x_1, \dots, x_{N_X}\}$  where  $x_j \in \mathbb{R}^3$  for  $j \in \{1, \dots, N_X\}$ . A point  $x_j$  consists of three components,  $x_j = \{x_j^x, x_j^y, x_j^z\}$ , which refer to the  $x$ ,  $y$ , and  $z$  components of the point, respectively. The transformation that maps a point  $x$  from the scene scan to the coordinate frame of the reference scan using a parameter estimate,  $p = [t_x, t_y, t_z, \phi, \theta, \psi]^T \in \mathbb{R}^3 \times \text{SO}(3)$ , is given as

$$T(p, x) = \begin{bmatrix} R_\phi R_\theta R_\psi & \\ & 1 \end{bmatrix} x + [t_x \ t_y \ t_z]^T$$

where  $R_\phi$  is the rotation matrix for a rotation about the  $x$  axis by angle  $\phi$ ,  $R_\theta$  is the rotation matrix for a rotation about the  $y$  axis by angle  $\theta$ ,  $R_\psi$  is the rotation matrix for a rotation about the  $z$  axis by angle  $\psi$ , and  $[t_x, t_y, t_z]^T$  is the translation vector between the two frames.

## III. PROPOSED METHOD

In order to improve the accuracy and convergence basin of the NDT algorithm, the Segmented Greedy Cluster NDT (SGC-NDT) method is proposed. The SGC-NDT method segments the ground points and performs clustering on the remaining points. Segmenting of the ground point and application of the greedy cluster algorithm is applied to both the point-to-distribution and distribution-to-distribution registration method for NDT.

The NDT algorithm is modified in three ways:

- 1) The ground points of the scan are removed using the ground segmentation method described in Section IV. In environments such as a large outdoor field, the collection of ground points are redundant and do not provide as much information for the purpose of scan registration as other environmental features such as large trees, fences, etc. Scan point density also becomes an issue as the ground points very close to the laser sensor are far denser than those farther away, which is not desirable for NDT as the high density of points near the vehicle will have a tendency to generate Gaussian distributions biased towards the sensor origin. The biased distribution effect can be somewhat mitigated using a down-sampling voxel based filter, however the filtering adds additional computation to the scan registration and removes information from the entire scan. Although down sampling the scan can mitigate the biased distribution issue for NDT, it does not solve the problem of the discontinuous cost function.
- 2) The non-ground points are clustered using the greedy clustering method described in Section V. By performing the clustering step, natural features in the environment, such as trees and bushes, are clustered to form the Gaussian distributions for SGC-NDT. In contrast, NDT performs a voxel based discretization, generating truncated Gaussian distributions which do not necessarily correctly model the environment.
- 3) To accommodate the greedy clustering style of clustering of the scan, the NDT cost calculation is modified as described in Section VII. NDT evaluates the Gaussian distribution within the cell that a transformed point falls into. The SGC-NDT algorithm evaluates the transformed point at all the Gaussian distributions for the clusters identified by the greedy clustering method. Similarly for distribution-to-distribution matching NDT, each Gaussian distribution in the scene scan is scored against all Gaussian distributions from the reference scan. Evaluation at all Gaussian components is computationally feasible, since the number of clusters identified in the scan is typically significantly smaller than the number of Gaussian distributions that would result from voxel based discretization. Calculating the cost based on all Gaussian distributions in the scans allows for the strongest contributions to come from the most likely clusters and provides a continuous

and differentiable cost function for the optimization.

#### IV. GROUND SEGMENTATION

The basis for the ground segmentation algorithm used for this work was first demonstrated by Douillard et al. [12]. Their method performs ground segmentation based on a 2D Gaussian process (GP) model of the sparse point clouds, which provides a probabilistic framework to identify ground points using an incremental sample consensus (INSAC) method. A modified version of Douillard's ground segmentation algorithm was introduced by Tongtong et al. [15]. To reduce computation, Tongtong divides the scan into sectors based on a polar grid binning, and applies the ground segmentation to each sector separately. The Gaussian process regression is formulated as an approximation based on the points contained in each sector. Tongtong's method was shown to run faster than the 2D method, with comparable results in segmentation quality. The 1D approximation method for ground segmentation from [15] is used in this work, and is briefly summarized in this section.

In order to perform the polar grid binning, the  $xy$  plane of the laser scan, in the laser frame, is first segmented into  $N_s$  angular sectors, where the  $i^{th}$  angular sector is denoted as  $\xi_i$ . Each sector is further sub-divided into  $N_b$  linear range based bins, which subdivides a sector as  $\xi_i = \{\xi_i^1, \dots, \xi_i^{N_b}\}$ . Finally, the points located within the  $j^{th}$  bin of the  $i^{th}$  sector, from scan  $Y$ , are denoted as  $(s_i^j)^Y = \{y \in Y : y \in \xi_i^j\}$  for all  $i \in \{1 \dots N_s\}$  and for all  $j \in \{1 \dots N_b\}$ . Denote the set  $S_Y$  as the collection of all individual point sets  $(s_i^j)^Y$ , and the function which accepts a scan  $Y$  and returns the collection of polar binned grid sets,  $S_Y$ , as  $S_Y = \tau(Y)$ .

The goal of ground segmentation for the 3D point cloud is to assign each point as either belonging to the ground or not ground. In this work, ground segmentation is done by performing Gaussian Process (GP) regression. In the case of terrain modelling, GP's are non-parametric tools which can be used to learn a model for the ground terrain. For a thorough exploration of the usage of GP's for ground terrain modelling, the reader is directed to the work of Vasudevan et al. [11]. In this work, the approximate GP regression method as described in [15] is applied. An example of the ground segmentation results for a representative laser scan is given in Figure 1. Denote the function which accepts a set of radial bins,  $S_Y$  and returns the non-ground points,  $Y'$ , as  $Y' \subset Y = \chi(S_Y)$ .

#### V. CLUSTERING OF THE NON-GROUND POINTS

Once the ground points have been segmented, the remaining non-ground points must be clustered in order to apply the SGC-NDT algorithm, which is achieved using a greedy clustering technique. For a scan  $Y$ , denote a cluster as  $\omega \subset Y$ , and the set of clusters as  $\Omega_Y = \{\omega_1 \dots \omega_{N_\Omega}\}$ , where  $N_\Omega$  is the total number of clusters, which is initially unknown. The clusters are generated by first randomly sampling an initial bin  $\tilde{s}_i^j \in S_Y$  from a random uniform distribution  $\mathcal{U}$ , such that  $\tilde{s}_i^j \sim \mathcal{U}(S_Y)$ . Note that  $S_Y$  is constructed from the polar binning of the non ground points from the 3D

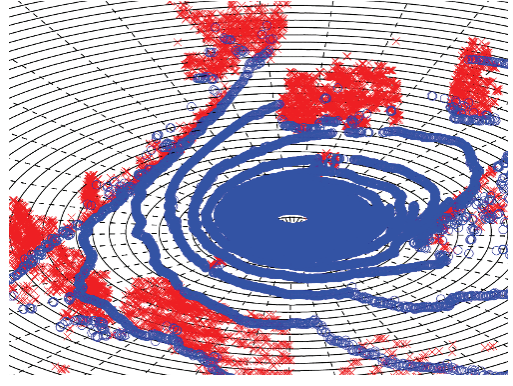


Fig. 1. Ground segmentation results for an outdoor scene with large trees and shrubs. Blue points have been classified as ground, and red points are classified as non-ground.

laser scan. Denote a nearest neighbour function  $\Theta_{S_Y}$ , which returns the set of eight neighbouring bins from  $\tilde{s}_i^j$  as the set  $\{\tilde{s}_{i+p}^{j+q} \setminus \tilde{s}_i^j \text{ for all } p \in \{-1, 0, 1\} \text{ and } q \in \{-1, 0, 1\}\}$ .

The nearest neighbours for  $\tilde{s}_i^j$  are generated and added to an ordered list of nearest neighbour bins,  $Q_{nn}$ . A bin in  $Q_{nn}$  can be compared against  $\tilde{s}_i^j$  to determine if the two can be combined. Merging of the bins is decided using the  $\Phi(\tilde{s}_i^j, Q_{nn}^k)$  function, where  $\Phi : S_Y \times S_Y \mapsto \{0, 1\}$ , and  $Q_{nn}^k$  is the  $k^{th}$  element of the list  $Q_{nn}$ . The  $\Phi$  function returns 1 if the two bins can be combined, and 0 otherwise. In the  $\Phi$  function, different metrics can be used to compare the point bins, such as Euclidean distance between the mean of the points contained in the bins, the L2 distance between Gaussian distributions within each bin, or a test for Gaussian fit. If the bins can be combined, the neighbour bin is added to an open list of bins,  $Q_o$ . The neighbour bin is also removed from the set of all bins,  $S_Y$ , and added to the current cluster,  $C_{cur}$ . The nearest neighbours of the bins from  $Q_o$  are explored and evaluated. When a bin is explored, its nearest neighbours are also added to  $Q_o$  based on the evaluation function  $\Phi$ . Once  $Q_o$  is empty, it means no further nearest neighbours can be assigned to the current cluster so a new bin from  $S_Y$  is selected, and the process is repeated. The entire process continues until all bins in  $S_Y$  have been assigned to a cluster. An example of the resulting Gaussian distributions after the greedy clustering has been completed is presented in Figure 2. Denote the function which accepts non ground points,  $Y'$ , and returns the set of clusters  $\Omega_Y$ , as  $\Omega_Y = \beta(Y')$ .

#### VI. THE NORMAL DISTRIBUTIONS TRANSFORM

The normal distributions transform is a method by which sections of a point cloud are mapped and represented as Gaussian distributions within a grid structure. The NDT registration algorithm begins by subdividing the space occupied by the reference scan into a set of grid cells,  $c$ . Denote the collection of reference scan points in cell  $c_i$  as  $Y^{c_i} = \{y_1^{c_i}, \dots, y_{N_{c_i}}^{c_i}\}$  such that  $y_k^{c_i} \in c_i$  for  $k \in \{1, \dots, N_{c_i}\}$ . The distribution of points within each cell,  $c_i$ , are modelled as Gaussian with a mean,  $\mu_{c_i}$ , and a covariance matrix,  $\Sigma_{c_i}$ . The Gaussian distribution represents a generative process that



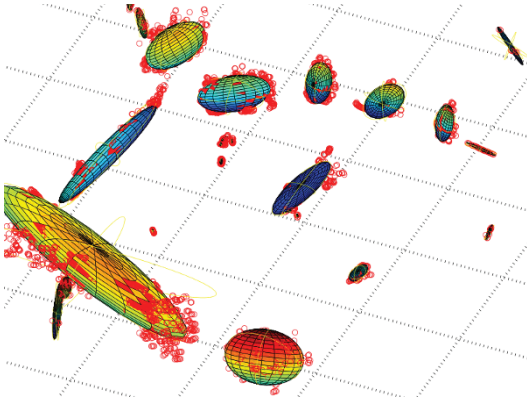


Fig. 2. The resulting Gaussian distributions after performing the greedy cluster algorithm on the non-ground point laser scan. One-sigma Gaussian distributions are shown (best viewed in colour).

models the local surface points  $Y^{c_i}$  within the cell.

Since the point cloud is modelled by a piecewise continuous and piecewise differentiable summation of Gaussians, numerical optimization tools can be used in order to register the scene scan with the reference scan. A fitness cost,  $\Lambda : \mathbb{R}^3 \times \text{SO}(3) \rightarrow \mathbb{R}$ , can be calculated which quantifies the measure of overlap between scans  $X$  and  $Y$ . The original work by Magnusson calculates the cost by evaluating each point in the transformed scan at the distribution corresponding to the NDT cell it occupies [16]. The score contribution for each point is given as

$$\rho(y) = \exp \left( -\frac{(y - \mu_{c_i})^T \Sigma_{c_i}^{-1} (y - \mu_{c_i})}{2} \right)$$

where  $\mu_{c_i}$  and  $\Sigma_{c_i}$  are the sample mean and covariance for cell,  $c_i$ . The sum of the score components for all points in the scan is known as the NDT point-to-distribution (p2d) cost, and is given as

$$\Lambda(p) = -\sum_{k=1}^{N_x} \rho_Y(T(p, x_k)).$$

Stoyanov et al. introduced a modified version of NDT which generates an NDT representation of both scans, then compares the distributions of the scans in order to align them [7]. The distribution-to-distribution cost function evaluates all pair-wise Gaussian components for both the scene and the reference scan. In Stoyanov's work however, the cost function is only evaluated at the nearest Gaussian component in order to reduce computation, which causes discontinuities in the overall cost function as the gradient and Hessian do not exist in the transformation space when the correspondences between mean points change. Discontinuities in the cost function are also present in point-to-distribution NDT, when scene scan points cross cell boundaries. Magnusson et al. address the cost discontinuity using a tri-linear interpolation scheme [17], however, interpolation does not fully solve the issue, as the cost functions are still discontinuous.

It should be noted that both NDT cost functions have analytic expressions available for calculation of the gradient,  $\eta_g$ , and Hessian,  $\eta_H$ . For point to distribution matching,

denote the functions  $\rho_g(x_k, p)$ , and  $\rho_H(x_k, p)$ , which use a point in the scene scan and the transformation parameters to calculate an associated gradient and Hessian contribution for point  $x_k$ . The optimization is initialized from a parameter estimate,  $p_0$ , and terminates once the norm of the gradient  $\|\eta_g\| \in \mathbb{R}$  is less than a user specified threshold,  $\epsilon$ . Stoyanov solves the optimization using a quasi-Newton approach with line search [7], however other approaches such as a Broyden-Fletcher-Goldfarb-Shanno (BFGS) update method can be used.

## VII. SEGMENTED GREEDY CLUSTER NDT

Using the Gaussian distributions generated by the greedy clustering, the NDT algorithm is modified to evaluate the cost function using all of the Gaussians. A summary of the SGC-NDT-P2D is given in Algorithm 1. For SGC-NDT-D2D, a method similar to the P2D version is applied, except in the D2D case both laser scans are segmented and clustered, and the set of resulting Gaussian distributions for each scan are compared to perform the registration.

---

**Algorithm 1** Register scene scan  $X$  with reference scan  $Y$  using SGC-NDT-P2D algorithm

---

```

1:  $S_X \leftarrow \tau(X)$ 
2:  $S_Y \leftarrow \tau(Y)$ 
3:  $X' \leftarrow \chi(S_X)$ 
4:  $Y' \leftarrow \chi(S_Y)$ 
5:  $\Omega_Y \leftarrow \beta(Y')$ 
6:  $p \leftarrow p_0$ 
7: while  $\|\eta_g\| > \epsilon$  do
8:    $\Lambda \leftarrow 0$ 
9:    $\eta_g \leftarrow 0$ 
10:   $\eta_H \leftarrow 0$ 
11:  for all  $x_k \in X'$  do
12:     $\bar{x}_k \leftarrow T(p, x_k)$ 
13:    for all  $\omega_j \in \Omega_Y$  do
14:       $\Lambda \leftarrow \Lambda + \rho(\bar{x}_k)_{\omega_j}$ 
15:       $\eta_g \leftarrow \eta_g + \rho_g(\bar{x}_k, p)_{\omega_j}$ 
16:       $\eta_H \leftarrow \eta_H + \rho_H(\bar{x}_k, p)_{\omega_j}$ 
17:    end for
18:  end for
19:   $\Delta p \leftarrow (\eta_H)^{-1}(\eta_g)$ 
20:   $p \leftarrow p + \Delta p$ 
21: end while
```

---

## VIII. EXPERIMENTAL RESULTS

The SGC-NDT approach is evaluated using two data sets of different environments and is compared against other scan registration algorithms. The algorithms used for comparison are ICP, NDT and G-ICP. For the purposes of comparison, the Point Cloud Library (PCL) implementations of ICP, NDT, and G-ICP are used [18]. The ICP algorithms are implemented using a maximum correspondence distance of 10m and the NDT algorithm was implemented with a grid size of 3m. For all optimization based approaches, the optimization is terminated when the norm of the gradient or the norm of the step size falls below  $10^{-6}$ .

### A. Accuracy in Outdoor Urban Environments

In order to test the accuracy of SGC-NDT against other scan registration methods, the Ford Campus Vision and LIDAR Data Set [14] is used. The data set was generated using a Velodyne HDL-64E LIDAR with ground truth acquired by integrating the high quality velocity and acceleration measurements produced by a Applanix POS-LV 420 INS with Trimble GPS. When scans were aligned using the ground truth measurements, the alignment was seen to have on the order of sub-degree accuracy in orientation and decimeter accuracy in position. Each algorithm performs pair-wise scan registration using every 10<sup>th</sup> scan produced by the LIDAR. The registration is initialized with a parameter estimate of zero translation and zero rotation. The error in the translation and rotation of registration is then compared against the ground truth measurements. The translational and rotational error distributions are displayed in Figure 3. It should be noted that the the upper adjacent and lower adjacent whiskers of the box-plots represent  $1.5 \times$  the interquartile range of the data.

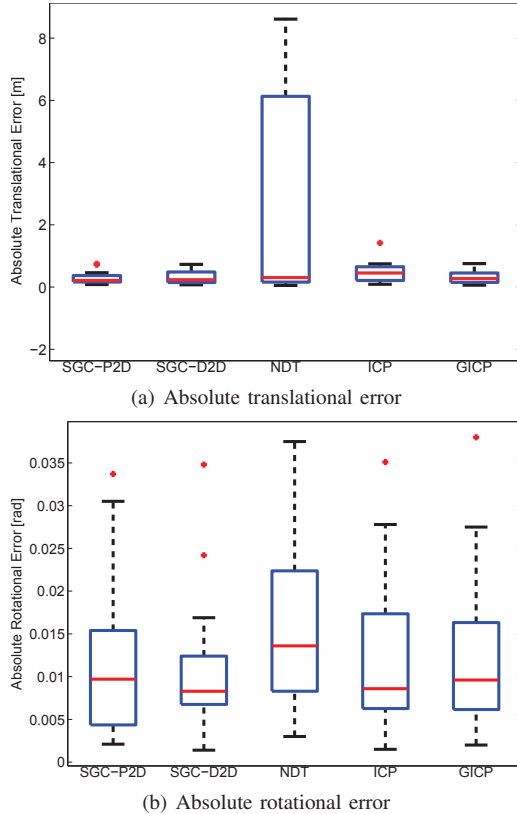


Fig. 3. Box-plots of the error distributions for each algorithm for the experiment from the Ford campus data set. (a) Absolute translational error. (b) Absolute rotational error

The error distributions from Figure 3 demonstrate that both SGC-NDT algorithms produce accurate results when compared against the ground truth, as does the G-ICP algorithm. The large translational error distribution for NDT demonstrates the algorithm's poor convergence characteristics, as the optimization has a tendency to converge to local minima.

TABLE I

SUMMARY OF CRISPNESS MEASURES FOR REGISTRATION TESTS IN URBAN AND FORESTED.

	ICP	G-ICP	SGC-NDT-P2D	SGC-NDT-D2D
<b>Ford</b>	132507	124911	125767	125221
<b>WPI</b>	-	44609	41884	40560

The ICP algorithm also shows fairly low translational and rotation errors, however, does not appear to be as accurate as SGC-NDT or G-ICP.

To further assess the scan registration quality, the pair-wise registered scans are aggregated into a global map. The maps are evaluated using a *crispness* measure, which is also used for map evaluation in [10]. The crispness of a map is evaluated by discretizing the 3D space into voxels, and recording the number of occupied voxels. For the experiment, a voxel size of 0.1 m is used. A map which evaluates to a lower number is said to be crisper than a map which evaluates to a higher number. Intuitively, the crispness quality measure captures the blurring of the map caused by incremental pair-wise registration errors as the scans are aggregated. The crispness measure is evaluated for SGC-NDT, ICP and G-ICP. A crispness for NDT is not evaluated since the registration did not converge to the global minimum on numerous occasions. The crispness measures for SGC-NDT, ICP and G-ICP are presented in Table I.

The crispness measures indicate that both SGC-NDT algorithms and G-ICP generate high quality maps, while ICP produces a lesser quality map due to the accumulation of registration error.

### B. Accuracy in Sparse Forested Environments

To determine the robustness of the proposed method, an experiment is performed using a dataset collected from a sparse, forested environment. The data was collected as part of the *NASA Sample Return Robot Challenge*, at Worcester Polytechnic Institute (WPI). The laser scans were collected using a Velodyne HDL-32E LIDAR, mounted to a custom made chassis designed for the challenge. The environment consists mainly of trees and other foliage, as well as a single small gazebo structure. Forested environments are specifically challenging for registration because foliage, grass and bush tend to create irregular, noisy point clouds with an ambiguous local surface, resulting in difficulties determining correct point correspondences and accurate surface normal information.

To determine robustness across all types of environments, only the two best performing algorithms, SGC-NDT and G-ICP, from the previous urban scenario experiment are presented, as the ICP and NDT algorithms were unable to converge consistently and do not provide any meaningful results for comparison. The experiment is performed in a similar manner to the urban scenario experiment, where scans are pair-wise registered using the competing algorithms. The registered scans are then aggregated into a global map. Each algorithm performs pair-wise scan registration using every 50<sup>th</sup> scan produced by the LIDAR, as the robot moved slowly through the environment. The registration is

initialized with a parameter estimate of zero translation and zero rotation. Visually, the result of aggregating the registered scans is presented in Figure 4. The experiment demonstrates performance in situations where odometry estimates are highly inaccurate, such as in GPS denied environments, or on vehicles where wheel slip or other factors make accurate state estimation difficult. Since accurate ground truth is not available for the WPI data set, the global maps are evaluated based solely on the crispness measure. The crispness measures for the WPI data set are presented in Table I.

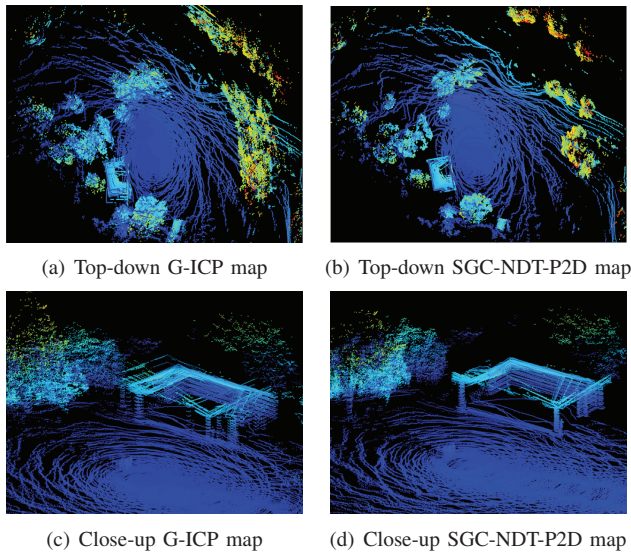


Fig. 4. Top-down and close up views for the resulting global maps using the SGC-NDT-P2D and G-ICP algorithms. (Best viewed in colour).

The crispness measure illustrates that G-ICP was not able to provide accurate scan registration results as compared to the SGC-NDT algorithms. The difficulty with convergence is most likely because G-ICP relies on accurate surface normals to determine the correct point correspondences, which is difficult to achieve in a forested environment. The SGC-NDT algorithm models environmental features such as trees and shrubs as a mixture of Gaussian distributions, thus good registration results are achievable in sparse environments with poor local surface structure. Figure 4 shows the maps from top down view of the traversed area, as well as a close up view of the environmental features. The G-ICP map shows significant drift and occasionally poor convergence to local minima, while the SGC-NDT map maintains very crisp features. The crispness of the features can be clearly identified by inspecting the alignment of the structural columns seen in the close-up view.

## IX. CONCLUSION

This work presents the segmented greedy cluster NDT, a modified version of the NDT algorithm. The proposed method segments the ground from the scans, clusters the non-ground points using a greedy cluster algorithm and models each cluster as a Gaussian distribution. The NDT scan registration algorithm is modified to use the clustered

Gaussians, as opposed to the standard NDT algorithm where the Gaussian clusters are generated from a voxel grid. The SGC-NDT approach is applied to both point to distribution and distribution to distribution NDT, and is shown to produce accurate results in both urban and sparse, forested environments. Future work involves using the Gaussian clusters as features for initial alignment of the scans, optimizing the implementation for real-time applications, a full analysis of computational complexity, and evaluating the algorithm in a larger set of environments.

## REFERENCES

- [1] P. Besl and H. McKay, "A method for registration of 3-d shapes," *IEEE Transactions on Pattern Analysis and Machine Intelligence*, vol. 14, no. 2, pp. 239–256, Feb 1992.
- [2] Y. Chen and G. Medioni, "Object modeling by registration of multiple range images," in *1991 IEEE International Conference on Robotics and Automation (ICRA)*, vol. 3, Sacramento, CA, USA, Apr 1991, pp. 2724–2729.
- [3] Z. Zhang, "Iterative point matching for registration of free-form curves and surfaces," INRIA-Sophia Antipolis, Tech. Rep., 1992.
- [4] A. Segal, D. Haehnel, and S. Thrun, "Generalized-ICP," in *2009 Robotics: Science and Systems (RSS)*, Seattle, USA, June 2009.
- [5] P. Biber and W. Strasser, "The normal distributions transform: a new approach to laser scan matching," in *2003 IEEE International Conference on Robotics and Automation (ICRA)*, vol. 3, Las Vegas, NV, USA, Oct. 2003, pp. 2743–2748.
- [6] M. Magnusson, A. Lilienthal, and T. Duckett, "Scan registration for autonomous mining vehicles using 3D-NDT," *Journal of Field Robotics*, vol. 24, no. 10, pp. 803–827, 2007.
- [7] T. Stoyanov, M. Magnusson, and A. Lilienthal, "Point set registration through minimization of the l2 distance between 3D-NDT models," in *2012 IEEE International Conference on Robotics and Automation (ICRA)*, St. Paul, MN, USA, May 2012, pp. 5196–5201.
- [8] A. Das and S. Waslander, "Scan registration with multi-scale k-means normal distributions transform," in *to appear in 2012 IEEE International Conference on Intelligent Robots and Systems (IROS)*, Vilamoura, Algarve, Portugal, Oct 2012.
- [9] F. Moosmann, O. Pink, and C. Stiller, "Segmentation of 3d lidar data in non-flat urban environments using a local convexity criterion," in *2009 IEEE Intelligent Vehicles Symposium*, June 2009, pp. 215–220.
- [10] B. Douillard, A. Quadros, P. Morton, J. Underwood, M. De Deuge, S. Hugosson, M. Hallstrom, and T. Bailey, "Scan segments matching for pairwise 3d alignment," in *2012 IEEE International Conference on Robotics and Automation (ICRA)*, St. Paul, MN, USA, May 2012, pp. 3033–3040.
- [11] S. Vasudevan, F. Ramos, E. Nettleton, and H. Durrant-Whyte, "Gaussian process modeling of large-scale terrain," *Journal of Field Robotics*, vol. 26, no. 10, pp. 812–840, 2009.
- [12] B. Douillard, J. Underwood, N. Kuntz, V. Vlaskine, A. Quadros, P. Morton, and A. Frenkel, "On the segmentation of 3d lidar point clouds," in *2011 IEEE International Conference on Robotics and Automation (ICRA)*, Shanghai, China, May 2011, pp. 2798–2805.
- [13] D. Bertsekas, *Nonlinear Programming*. Athena Scientific, 1999.
- [14] G. Pandey, J. R. McBride, and R. M. Eustice, "Ford campus vision and lidar data set," *International Journal of Robotics Research*, vol. 30, no. 13, pp. 1543–1552, November 2011.
- [15] C. Tongtong, D. Bin, L. Daxue, Z. Bo, and L. Qixu, "3d lidar-based ground segmentation," in *2011 First Asian Conference on Pattern Recognition (ACPR)*, Beijing, China, Nov 2011, pp. 446–450.
- [16] M. Magnusson, "The three-dimensional normal-distributions transform — an efficient representation for registration, surface analysis, and loop detection," Ph.D. dissertation, Örebro University, Dec. 2009, Örebro Studies in Technology 36.
- [17] M. Magnusson, T. Duckett, and A. J. Lilienthal, "Scan registration for autonomous mining vehicles using 3D-NDT," *Journal of Field Robotics*, vol. 24, no. 10, pp. 803–827, Oct 24 2007.
- [18] R. B. Rusu and S. Cousins, "3D is here: Point Cloud Library (PCL)," in *2011 IEEE International Conference on Robotics and Automation (ICRA)*, Shanghai, China, May 9–13 2011, pp. 1–4.